Demonstration of a Quasi-Gapless Integrated Visible Light Communication and Positioning System

Helin Yang, *Student Member, IEEE*, Chen Chen, Wen-De Zhong, *Senior Member, IEEE*, Arokiaswami Alphones, *Senior Member, IEEE*, Sheng Zhang, and Pengfei Du

***Abstract*— In this letter, a quasi-gapless integrated visible light communication and positioning (VLCP) system is experimentally demonstrated for the first time based on filter bank multicarrier-based subcarrier multiplexing (FBMC-SCM). Compared with orthogonal frequency division multiplexing-based SCM (OFDM-SCM), FBMC-SCM has lower out-of-band interference and, therefore, requires much smaller guard band (GB) spacing. A low-complexity transmit diversity transmission scheme is adopted here, where all the light emitting diode lamps transmit the same communication signal. Moreover, phase difference of arrival is applied for positioning. The experimental results show that, in a coverage area of 1.2 × 1.2 m^2 with a height of 2.1 m, the mean position errors using OFDM-SCM and FBMC-SCM for a GB of 0.7 MHz are 10.91 and 6.08 cm, respectively. Moreover, a comparable bit-error-rate performance can be achieved for both OFDM-SCM and FBMC-SCM. Due to the negligible GBs when using FBMC-SCM, the effective bandwidth utilization ratio of the integrated VLCP system is improved from 72% to 98% when OFDM-SCM is replaced by FBMC-SCM.**

***Index Terms*— Visible light communication and positioning, filter-bank multicarrier, subcarrier multiplexing.**

I. Introduction

WHITE light emitting diodes (LEDs) have grown rapidly in the lighting market and will replace traditional light sources owing to their attractive characteristics such as high brightness, long lifetime, high energy efficiency and low cost [1]. Besides illumination, LEDs can also be applied for visible light communication (VLC) or visible light positioning (VLP). On the one hand, white LEDs based VLC has been emerging as a promising technique for indoor wireless communications, due to its many distinctive advantages such as low-cost front-ends, abundant unregulated bandwidth, high security, etc. [2]. So far, many techniques have been proposed to increase the capacity of bandlimited VLC systems, such as multiple-input multiple- output, orthogonal frequency division multiplexing (OFDM) and frequency domain equalization [3]–[5]. On the other hand, VLP using white LEDs has attracted great attention in recent years, because of its high positioning accuracy, low cost and guaranteed security in comparison to the radio frequency (RF) based indoor positioning systems [6]. To date, many algorithms have been applied in VLP systems, such as received signal strength (RSS), time of arrival (TOA), angle of arrival (AOA), time difference of arrival (TDOA), and phase difference of arrival (PDOA) [6]–[9]. Among them, PDOA has been shown to achieve high accuracy within a practical coverage area [10].

In practical indoor environments, high-speed communication and high-accuracy positioning might be expected at the same time in certain scenarios (such as supermarket, hospital, robotic industry, etc.), and therefore the integration of VLC and VLP can be performed to provide simultaneous communication and positioning for indoor users. However, such integrated systems have not yet be adequately investigated and only several works have been reported so far. Specifically, the combination of OFDM modulation and RSS algorithm has been proposed for the integration of VLC and VLP in [11]–[13]. Nevertheless, due to the sensitivity to the variation of light intensity, it might be challenging for RSS-based VLP systems to achieve high positioning accuracy. Moreover, OFDM signals usually have relatively high out-of-band interference (OOBI), which might also degrade the performance of the integrated system.

To address the above issues, we have proposed an integrated VLC and VLP (VLCP) system using filter bank multicarrier-based subcarrier multiplexing (FBMC-SCM) and PDOA in our previous work [14]. It has been verified by our preliminary simulation results that the VLCP system using FBMC-SCM requires much reduced guard bands (GBs) in comparison to that using OFDM-SCM, and therefore achieves a higher spectral efficiency and improved positioning accuracy. In [14], different LEDs are used to transmit different communication subbands and multiple bandpass filters (BFPs) are required to separate these subbands before demodulation, which results in relatively high implementation complexity. Moreover, only simulation results have been reported and no experimental validations have been conducted yet.

In this letter, we experimentally demonstrate a quasi-gapless integrated VLCP system based on FBMC-SCM and PDOA. In order to reduce complexity of the system, a transmission diversity scheme is adopted, where all the LEDs are used to transmit the same communication signal. Experiments have been conducted to verify the feasibility of integrated VLCP systems and the comparison between FBMC-SCM and OFDM- SCM has also been performed. The experimental

Manuscript received August 26, 2018; revised September 23, 2018; accepted October 3, 2018. Date of publication October 8, 2018; date of current version November 20, 2018. This work was supported in part by Delta Electronics Inc., and in part by the National Research Foundation, Singapore, under the Corporate Laboratory@University Scheme. *(Corresponding author: Chen Chen.)*

The authors are with the School of Electrical and Electronic Engineering, Nanyang Technological University, Singapore 639798 (e-mail: hyang013@e.ntu.edu.sg; chen0884@e.ntu.edu.sg).

Color versions of one or more of the figures in this letter are available online at http://ieeexplore.ieee.org.

Digital Object Identifier 10.1109/LPT.2018.2874311

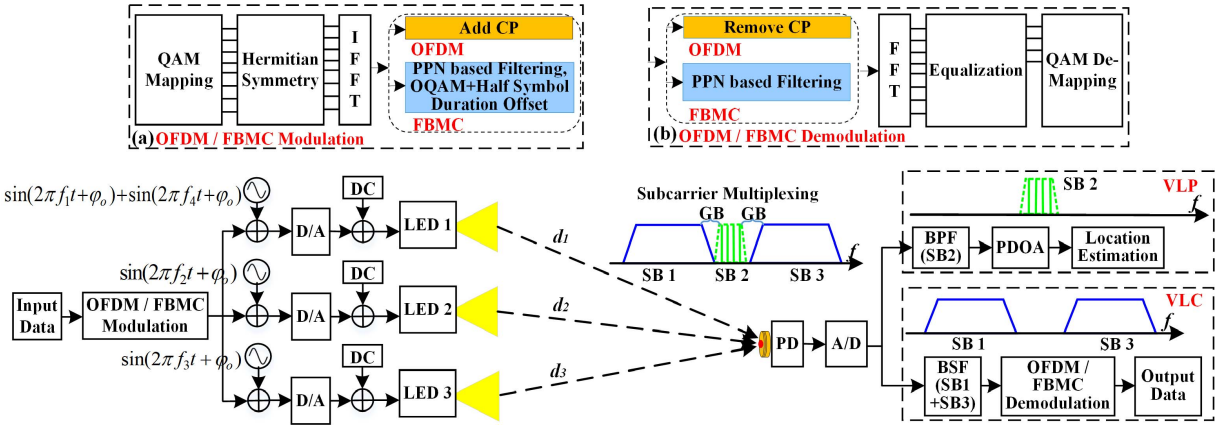

Fig. 1. Block diagram of the integrated VLCP system. Insets: principle of OFDM/FBMC (a) modulation and (b) demodulation. (SB: subband).

results show that simultaneous communication and positioning can be achieved in the integrated VLCP system. Moreover, the system using FBMC-SCM attains a greatly improved positioning accuracy than that using OFDM-SCM, while maintaining a comparable bit error rate (BER) performance. It is further verified that negligible GBs are required in integrated VLCP systems using FBMC-SCM, which can improve the effective bandwidth utilization ratio compared with OFDM-SCM.

II. Integrated VLCP System

In practical indoor environments, a number of LED lamps are usually installed to set up a VLC system to satisfy lighting requirements and to provide data communication and estimate the location of an indoor user. The LED lamps generally use the intensity modulation with direct detection (IM/DD), where the intensity of each LED lamp is modulated with the transmitted data and a photodetector (PD) is used to convert the light into an electrical signal. In the integrated VLCP system, we apply two-dimensional (2D) PDOA-based positioning at the receiver to estimate the locations of indoor users [10].

A. PDOA-Based Positioning

The block diagram of the integrated VLCP system is shown in Fig. 1, where three LED lamps are adopted at the transmitter side and one PD is used at the receiver side. To implement the PDOA-based positioning, three LED lamps are synchronized and modulated with four sinusoidal signals with four different frequencies, where f_1 and f_4 are both modulated to LED 1, while f_2 and f_3 are modulated to LED 2 and LED 3, respectively. Let d_i be the distance between the i-th ($i = 1, 2, 3$) LED lamp and the PD. It has been shown in [10] that there exists the position shifting effect in practical PDOA-based VLP systems caused by the nonuniform initial time delay pattern of the commercial off-the-shelf LEDs, which can be efficiently mitigated by the neural network-based post-compensation approach.

At the receiver, the differential PDOA algorithm is executed and finally two distance differences, i.e., d_1-d_2 and d_2-d_3, can be obtained. Given the locations of the three LED lamps and the distance differences, the position of the user can be successfully estimated. The detailed procedures to implement PDOA-based positioning can be found in [10].

B. FBMC/OFDM-SCM

Insets (a) and (b) in Fig. 1 present the principle of modulation and demodulation of OFDM/FBMC, respectively. In order to reduce the large OOBI, FBMC applies a prototype filter to filter each subcarrier. The principles of the two modulation schemes are the same, except that the CP insertion in OFDM is replaced by the polyphaser network (PPN) based filtering in FBMC [15]. As shown in Fig. 1(a), after quadrature amplitude modulation (QAM) mapping, Hermitian symmetry is imposed before the inverse fast Fourier transform (IFFT) so as to generate a real- valued signal. To guarantee the orthogonality between adjacent subcarriers, offset QAM (OQAM) with a half-symbol-duration offset is applied [15].

For the generation of FBMC signals, the Mirabbasi-Martin filter (MM-filter) is applied and the filter function is given by

$$H(f) = \sum_{k=-(K-1)}^{K-1} H_k \frac{\sin\left(\pi(f - k/MK)MK\right)}{MK \sin\left(\pi(f - k/MK)\right)} \qquad (1)$$

where K is the overlapping factor, H_k is the coefficient used to control the out-of-band filter frequency response, and M is the IFFT/FFT size [16].

As can be seen from Fig. 1, the total modulation bandwidth of the integrated VLCP system is divided into three subbands with two GBs. Specifically, subbands 1 and 3 are used for VLC while subband 2 is reserved for PDOA positioning. In addition, the two GBs are assumed to have the same frequency spacing. It should be noted that all the LED lamps are used to transmit the same OFDM/FBMC-encoded communication signal which is carried by subbands 1 and 3. By adopting such a transmit diversity transmission scheme, the implementation complexity can be reduced compared with our previous scheme in [14]. Before digital-to-analog conversion (D/A), the sinusoidal signals for VLP and the OFDM/FBMC signal for VLC are added together with respect to each LED lamp. Subsequently, direct current (DC) biases are added and the resultant signals are utilized to drive the three LED lamps, respectively. The sinusoidal signals for VLP are synchronized at the transmitter.

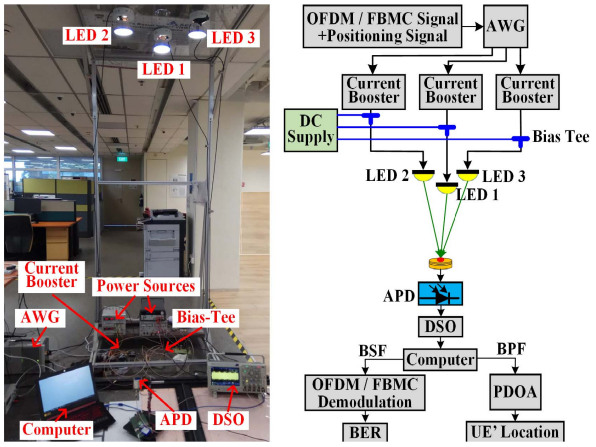

Fig. 2. Experimental setup of the integrated VLCP system.

At the receiver side, the optical signal is detected by the PD and converted to an electrical signal. On one hand, subband 2 which contains the positioning signal can be obtained by using a BPF and the location of the user can be calculated according to the PDOA algorithm [10]. On the other hand, subbands 1 and 3 containing the communication signal can be achieved with a band stop filter (BSF) and OFDM/FBMC demodulation is then applied to recover the communication data. Hence, both the communications and positioning purposes can be achieved in this integrated VLCP system.

III. Experimental Setup and Results

In this section, we present the experimental results to verify the feasibility of the integrated VLCP system within a practical indoor environment. The experimental setup of the integrated VLCP system is depicted in Fig. 2. Both the OFDM/FBMC signal for VLC and the sinusoidal signals for VLP are offline generated using MALTAB, which are then uploaded to a multi- channel arbitrary waveform generator (AWG, Spectrum M4x. 6622-x4) with a sampling rate of 100 MSa/s. After amplifying and adding DC biases, the obtained signals are used to drive three LED lamps (Lumileds LXML-PWCI). After free-space propagation, the light is captured by an avalanche PD (APD, Hamamatsu S8664-50K) after passing by a blue filter (BF). The detected signal is recorded by a digital storage oscilloscope (Tektronix MDO3104) with a sampling rate of 100 MSa/s. Subsequently, the demodulation of the communication signal and the estimation of the user's location are executed offline using MALTAB. To extend the modulation bandwidth, digital pre-frequency domain equalization is used in the system [17].

We test the performance of the integrated VLCP system in a quarter area of 1.2 m × 1.2 m and the vertical distance between the LED lamps and the PD is 2.1 m. The locations of three LED lamps are (0, −0.175, 2.1), (0.25, 0.075, 2.1) and (−0.25, 0.075, 2.1) with the origin (0, 0, 0), where the units are all meters. The APD has an active area of 19.6 mm^2 and a responsivity of 15

A/W at the wavelength of 450 nm. The system modulation bandwidth is extended to 10 MHz and 4-QAM mapping is used for communication. For both OFDM and FBMC,

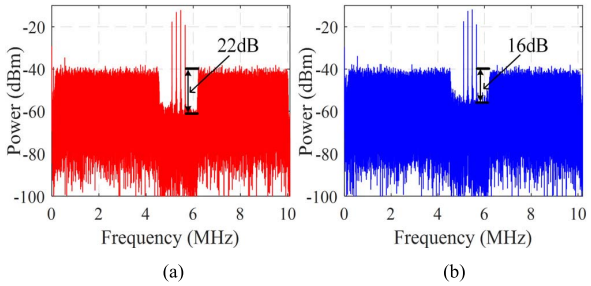

Fig. 3. Received spectra of (a) FBMC-SCM signal and (b) OFDM-SCM signal.

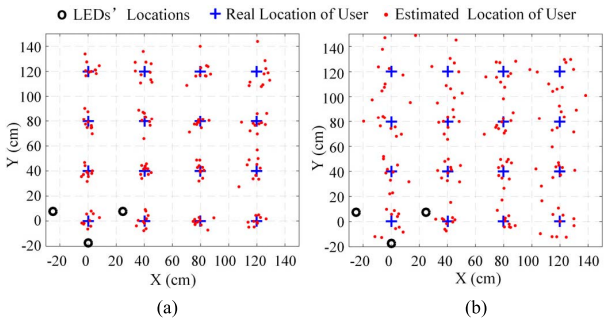

Fig. 4. Positioning results based on (a) FBMC-SCM and (b) OFDM-SCM.

the IFFT/FFT size is 512, and the number of data subcarriers is 51. The overlapping factor in FBMC is set to $K = 4$. The frequencies of the four sinusoidal signals for positioning are in the range between 5.1 to 5.7 MHz with a frequency gap of 0.2 MHz.

Figs. 3(a) and (b) show the received electrical spectra of the OFDM-SCM signal and the FBMC-SCM signal, respectively, where the GB spacing is 0.7 MHz. We can see that, compared with OFDM, the OOBI of FBMC is effectively suppressed, resulting in much reduced power leakage at the positioning frequency subband. A significant 6-dB OOBI reduction can be achieved by using FBMC-SCM in comparison to OFDM-SCM.

Figs. 4(a) and (b) demonstrate the positioning results over the testing area in the integrated VLCP system using FBMC-SCM and OFDM-SCM, respectively. The frequency spacing of GB is set to 0.7 MHz. As we can see, when the user is moving away from the LED lamps, the positioning accuracy is gradually deceased for both FBMC-SCM and OFDM-SCM. It can be clearly observed from Fig. 4 that a higher positioning accuracy is achieved by using FBMC-SCM compared with OFDM-SCM over the 1.2 m × 1.2 m coverage area. For FBMC-SCM, most of the positioning errors are less than 8 cm and only a few of them are more than 10 cm when the user is at edge of the coverage area, and the mean position error is 6.08 cm. However, for OFDM-SCM, the positioning errors are mainly ranging from 7 to 20 cm, and only a few of them are below 5 cm when the user is at center of the coverage area, and the mean positioning error is as high as 10.91 cm. Fig. 5 shows the cumulative distribution functions (CDFs) of the positioning errors using OFDM-SCM and FBMC-SCM. As can be seen, the positioning errors at 90% confidence for OFDM-SCM and FBMC-SCM are 19.6 and 11.2 cm, respectively, which indicates a positioning accuracy improvement of up to 8.4 cm.

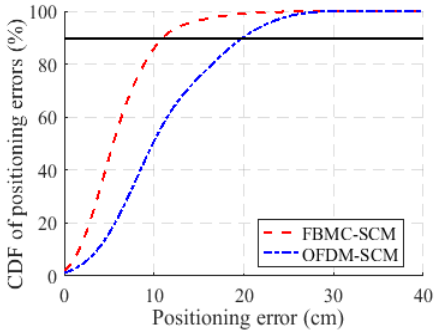

Fig. 5. CDF of positioning errors using OFDM-SCM and FBMC-SCM.

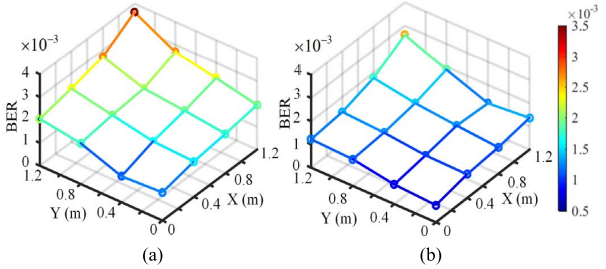

Fig. 6. BER distribution of (a) FBMC-SCM and (b) OFDM-SCM.

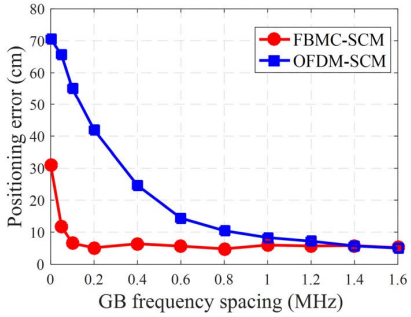

Fig. 7. Positioning error versus GB frequency spacing.

Fig. 6 shows the BER distribution over the testing area using OFDM-SCM and FBMC-SCM. It can be seen that the BER values over the testing area for both OFDM-SCM and FBMC-SCM are all less than 3.8×10^{-3}. More specifically, due to the adverse effect of subcarrier filtering in FBMC [16], the BER performance of FBMC-SCM is slightly worse than that of OFDM-SCM, but still remains at a comparable level.

Fig. 7 presents the positioning error versus the GB frequency spacing. For OFDM-SCM, the positioning error is gradually reduced as the GB frequency spacing is increased from 0 to 1.4 MHz. However, a rapid reduction of positioning error is shown for FBMC-SCM when the GB frequency spacing is increased from 0 to 0.1 MHz. We can observe that OFDM-SCM achieves nearly the same positioning accuracy as the FBMC-SCM only when the GB frequency spacing is larger than 1.4 MHz. To achieve the best positioning accuracy, OFDM-SCM requires a minimum GB frequency spacing of 1.4 MHz; however, FBMC- SCM only requires a negligible GB frequency spacing of 0.1 MHz. Defining the effective bandwidth utilization ratio (EBUR) as the ratio of the bandwidth occupied by the communication and positioning signals to the total modulation bandwidth, the EBURs using OFDM-SCM and FBMC-SCM to achieve the same positioning accuracy are 72% and 98%, respectively.

IV. Conclusion

In this letter, we have experimentally demonstrated an indoor integrated VLCP system based on the FBMC-SCM technique and the PDOA algorithm, which can efficiently provide both indoor communication and positioning functions. Experimental results show that FBMC-SCM can greatly reduce the OOBI in comparison to OFDM-SCM, which can avoid the need of large GB spacing, and hence improves the EBUR from 72% to 98% to achieve the same positioning accuracy with comparable BER performance. In conclusion, the demonstrated integrated VLCP system might be promising for future indoor environments.

References

[1] R. D. Dupuis and M. R. Krames, "History, development, and applications of high-brightness visible light-emitting diodes," *J. Lightw. Technol.*, vol. 26, no. 9, pp. 1154–1171, May 1, 2008.

[2] H. Haas, "Visible light communication," in *Proc. Opt. Fiber Commun. Conf. (OFC)*, 2015, Paper Tu2G.5.

[3] C. Chen, W.-D. Zhong, and D. Wu, "On the coverage of multiple-input multiple-output visible light communications [Invited]," *J. Opt. Commun. Netw.*, vol. 9, no. 9, pp. D31–D41, Sep. 2017.

[4] C.-H. Yeh, H.-Y. Chen, C.-W. Chow, and Y.-L. Liu, "Utilization of multi-band OFDM modulation to increase traffic rate of phosphor-LED wireless VLC," *Opt. Express*, vol. 23, no. 2, pp. 1133–1138, Jan. 2015.

[5] H. Le Minh *et al.*, "High-speed visible light communications using multiple-resonant equalization," *IEEE Photon. Technol. Lett.*, vol. 20, no. 14, pp. 1243–1245, Jul. 15, 2008.

[6] M. F. Keskin, A. D. Sezer, and S. Gezici, "Localization via visible light systems," *Proc. IEEE*, vol. 106, no. 6, pp. 1063–1088, Jun. 2018.

[7] H. Steendam, T. Q. Wang, and J. Armstrong, "Theoretical lower bound for indoor visible light positioning using received signal strength measurements and an aperture-based receiver," *J. Lightw. Technol.*, vol. 35, no. 2, pp. 309–319, Jan. 15, 2017.

[8] P. F. Du, S. Zhang, C. Chen, A. Alphones, and W.-D. Zhong, "Demonstration of a low-complexity indoor visible light positioning system using an enhanced TDOA scheme," *IEEE Photon. J.*, vol. 10, no. 4, May 2018, Art. no. 7905110.

[9] A. Naz, H. M. Asif, T. Umer, and B.-S. Kim, "PDOA based indoor positioning using visible light communication," *IEEE Access*, vol. 6, pp. 7557–7564, 2018.

[10] S. Zhang, W.-D. Zhong, P. Du, and C. Chen, "Experimental demonstration of indoor sub-decimeter accuracy VLP system using differential PDOA," *IEEE Photon. Technol. Lett.*, vol. 30, no. 19, pp. 1703–1706, Oct. 1, 2018.

[11] M. Aminikashani, W. Gu, and M. Kavehrad, "Indoor positioning with OFDM visible light communications," in *Proc. IEEE Consum. Commun. Netw. Conf. (CCNC)*, Jan. 2016, pp. 505–510.

[12] B. Lin, X. Tang, Z. Ghassemlooy, C. Lin, and Y. Li, "Experimental demonstration of an indoor VLC positioning system based on OFDMA," *IEEE Photon. J.*, vol. 9, no. 2, Apr. 2017, Art. no. 7902209.

[13] Y. Xu *et al.*, "Accuracy analysis and improvement of visible light positioning based on VLC system using orthogonal frequency division multiple access," *Opt. Express*, vol. 25, no. 26, pp. 32618–32630, Apr. 2017.

[14] H. Yang, C. Chen, W.-D. Zhong, S. Zhang, and P. Du, "An integrated indoor visible light communication and positioning system based on FBMC-SCM," in *Proc. IEEE Photon. Conf. (IPC)*, Oct. 2017, pp. 129–130.

[15] S.-Y. Jung, D.-H. Kwon, S.-H. Yang, and S.-K. Han, "Inter-cell interference mitigation in multi-cellular visible light communications," *Opt. Express*, vol. 24, no. 8, pp. 8512–8526, Mar. 2016.

[16] M. Bellanger *et al.*, "FBMC physical layer: A primer," *PHYDYAS*, vol. 25, no. 4, pp. 7–10, Jan. 2010.

[17] C. Chen, W.-D. Zhong, and D. Wu, "Indoor OFDM visible light communications employing adaptive digital pre-frequency domain equalization," in *Proc. CLEO*, 2016, pp. 1–2, Paper JTh2A.118.